Resonant ac Dipolar Excitation for Ion Motion Control in the Orbitrap Mass Analyzer

Qizhi Hu,[†] Alexander A. Makarov,[‡] R. Graham Cooks,[†] and Robert J. Noll*[,†]

Chemistry Department, Purdue University, West Lafayette, Indiana 47907, and Thermo Electron (Bremen), Hanna-Kunath-Strasse 11, Bremen 28199 Germany

Received: August 10, 2005; In Final Form: December 30, 2005

A dipolar ac signal applied to the split outer electrode of an Orbitrap mass spectrometer at the axial resonance frequency causes excitation of ion axial motion and either eventual ion ejection from the trap, if applied in phase with ion motion, or de-excitation, if applied 180° out of phase. Both de-excitation and excitation may be achieved mass-selectively. The extent of ion axial de-excitation depends on the ac amplitude and on the number of cycles applied; sufficient de-excitation can be accomplished such that the ion signal cannot be observed above baseline noise. After de-excitation, the ions remain trapped and in rapid orbital (but not axial) motion, which allows them to be re-excited coherently by application of a second ac waveform allowing the signal again to be observed. Both broad-band and narrow-band waveforms have been used to de-excite and to re-excite ion motion. Using narrow-band waveforms, selective de-excitation and re-excitation can be performed with unit mass selection, leaving an adjacent ^{13}C isotopic peak unaffected. The origin and potential applications of these new capabilities is delineated.

Introduction

The Orbitrap, a new mass analyzer based on the Kingdon trap,[1] consists of two specially shaped electrodes: a spindle-like inner electrode and a barrel-like outer electrode. A high dc voltage is applied between the inner and outer electrodes, creating an electric field separable into *r* and *z* (radial and axial) coordinates, so that the potential distribution $U(r, z)$ is given by

$$U(r,z) = \frac{k}{2}\left(z^2 - \frac{r^2}{2}\right) + \frac{k}{2}(R_m)^2 \ln\left[\frac{r}{R_m}\right] + C \qquad (1)$$

where C is a constant, k is proportional to the axial restoring force constant, and R_m is the characteristic radius. Stable ion trajectories involve both orbiting motion *around* the central electrode (r, φ-motion, where φ is the angular coordinate) and *simultaneous* oscillations in the z-direction. Orbital (radial) trapping is essential for confining the ions and it takes place for ion trajectories with $r < R_m$ but does not do so for $r \geq R_m$. Axial motion is the basis for mass analysis in this instrument. As is evident from eq 1, the specially shaped electrodes produce an electrostatic potential containing no cross terms in r and z.

Thus, the potential in the z-direction is exclusively quadratic. Ion motion along the z-axis may be described as a harmonic oscillator and it is completely independent of r, φ motion. The product of the parameter k (eq 1) times the ion charge, kq, is the force constant for the harmonic restoring force in the axial direction. The value of k is determined by the exact shape of the Orbitrap electrodes and the applied potential. (Here, we denote the ion charge by q, to avoid confusion with the z-coordinate.) The ion mass/charge ratio, m/q, is related to the frequency of ion motion along the z-axis by the velocity-independent expression[2]

$$\omega = [k(q/m)]^{1/2} \qquad (2)$$

The frequency is measured by broad-band ion image current detection, followed by use of a fast Fourier transform (FFT) algorithm[3] to convert the recorded time-domain signal into a mass/charge spectrum.[4] The outer electrode is split at the "equator" of the Orbitrap ($z = 0$ plane), forming two electrodes that detect the ion image current induced by axial motion. As Makarov has previously shown, the ion image current is proportional to the number of ions, N (at a given mass/charge ratio), as well as Δz, the axial amplitude of the ion motion, as given by the following expression,

$$I(t) = -qN\omega\frac{\Delta z}{\lambda}\sin(\omega t) \qquad (3)$$

where λ is a factor to account for the geometry of the Orbitrap electrodes.[2] When more than one mass-to-charge ratio is present in the Orbitrap, the ion current becomes a sum of expressions such as eq 3 for each mass/charge ratio. Although the radial and angular frequencies are also mass-dependent, the axial frequency is used because it alone is (to first order) completely independent of ion kinetic energy and of the spatial spread of the ions. High performance mass analysis, in terms of mass resolution and mass accuracy, can be achieved in the Orbitrap mass analyzer because of this energy independence.

The Orbitrap provides high mass resolution (up to 150 000), large space charge capacity, high mass accuracy (1−5 ppm),[5] a mass/charge ratio range of at least 6000 and a linear dynamic range of more than 3 orders of magnitude.[6] Although a powerful mass analyzer, better understanding of the fundamentals in this device, including the complexities of ion motion, are sought because such understanding offers the possibility to improve performance and to develop tandem mass spectrometry capabilities. These characteristics are necessary in meeting the chal-

* Corresponding author. Tel: 765-494-5265. Fax: 765-494-9421. E-mail: rnoll@purdue.edu.
† Purdue University.
‡ Thermo Electron (Bremen).

10.1021/jp054485v CCC: $33.50 © 2006 American Chemical Society
Published on Web 02/08/2006

lenges of modern analytical chemistry in such areas as genomics, proteomics, and metabolomics.

Comparisons of the Orbitrap and the quadrupole ion trap (3-D Paul trap) show many similarities. Although both electric potential distributions contain a dominant quadrupolar component, this somewhat superficial observation ignores an important distinction between the two devices, namely, the quadrupole ion trap is a radio frequency (RF) device whereas the Orbitrap operates with electrostatic fields (ignoring the initial electrodynamic squeezing used when introducing ions into the trap). Nonetheless, ion axial motion in the quadrupole ion trap can be reasonably well-approximated as an harmonic oscillator for Mathieu parameter (q_z) values < 0.4 with axial secular frequency (ω_z) by neglecting higher frequency ion micromotion.[7,8] Thus, the real similarity is that ion motion in the axial direction is harmonic for both devices; this conclusion is useful in the research described here. Furthermore, ion motion control experiments previously carried out on the quadrupole ion trap will serve as an important guide to controlling ion motion within the Orbitrap.

Ion motion control and diagnostic experiments on the quadrupole ion trap include resonant ac dipolar excitation[9−11] and short duration dc pulse excitations applied to the endcap electrodes.[12,13] Resonant dipolar excitation is performed in the quadrupole ion trap for the purposes of resonant ejection,[9,14] selective ejection for ion isolation,[15,16] and collision-induced dissociation (CID) by exciting ion translational kinetic energy.[17,18] Selective, broad-band excitation of ions in the ion trap has also been performed in experiments in which ions of a wide range of mass/charge ratios are excited.[19,20] Short symmetrical (potential applied to both end caps) or asymmetrical (potential applied to one end cap) axial dc pulses have been used to activate trapped ions to cause their ejection[21] or force them into coherent motion with characteristic secular frequencies.[22]

Tomography investigations, such as the pulse-pump/laser-probe experiment[23,24] in which photodissociation yields are monitored as a function of ion cloud axial position in the ion trap, have been used in earlier work from this lab to establish the positions, velocities, kinetic energies and frequencies of resonantly excited ions in the quadrupole ion trap. Still other tomography experiments have used a single short-duration dc pulse to investigate aspects of exact ion micromotion.[21] Finally, we note that dc pulses of this type—but usually of larger magnitude—have also been used to destabilize ion orbits, either radially or axially, to effect surface-induced dissociation (SID) upon collisions of ions with the electrodes in quadrupole ion traps.[13,25]

The rich diversity of experiments in the quadrupole ion trap suggests that a similar variety of analogous ion manipulation experiments could be carried out in the Orbitrap. These include studying the effects of resonant ac dipolar excitation and dc pulse activation using both symmetrical and asymmetrical pulses. dc pulse activation is of considerable interest, as typically this mode of excitation is very rapid, e.g., in causing trapped ion orbits to become unstable, either radially or axially. Also of interest, dipolar ac excitation,[26−28] impulsive excitation,[22] or broad-band SWIFT excitations[29] may be useful in the Orbitrap to force product ions into coherent motion.

This paper reports on a series of experiments performed on ions confined in the Orbitrap. These experiments demonstrate that ion motion in the *z*-direction can be controlled by applying ac waveforms to the two outer electrodes of the Orbitrap. These ac voltages applied are small (<20 V) compared to the harmonic axial potential well (500 V) but do create a time-varying electric field along the *z*-axis. Thus, ion axial motion may be modeled as a forced, undamped, harmonic oscillator, where the forcing function is proportional to the ac axial electric field. We note that none of the experiments cause significant changes in the radial motion; the ions remain trapped radially and that is all that is sought.

Consequently, excitation of an ion's axial motion can occur if the ac electric field is resonant (or nearly resonant) with the ion's characteristic axial frequency as given by eq 2; sufficient excitation will cause the ion to eject from the trap. On the other hand, if the time-varying electric field opposes ion motion, de-excitation of the axial motion will occur. In this case, the ion can thus be brought to rest at $z = 0$, with no motion in the z direction. Although *not* ejected from the trap, the ion has been brought to a "dark" state, as the ion signal is only generated by ions with nonzero *z*-axis amplitude (see eq 3). This result, detailed below, is not a peculiarity of the Orbitrap, but a general result for a forced undamped harmonic oscillator.

In this paper, we report on experiments involving ion axial excitation and de-excitation and examine the effects of the excitation waveform's (viz. time-varying axial electric field's) amplitude, bandwidth, and phase relative to ion axial motion, and the ability to control ion signals in a mass-selective fashion using tailored-waveforms. Simulations (SIMION 3D, Version 7[30] and ITSIM, research version[31,32]) of the effects of resonant dipolar ac excitation in the Orbitrap are used to provide supporting information.

Such capability to control ion axial motion in the Orbitrap is important for at least two reasons: (i) to perform tandem mass spectrometry (MS/MS) within the Orbitrap and (ii) to study and control ion packet axial extent and thereby improve Orbitrap performance. In the first case, ion activation methods, especially such as blackbody-induced radiative dissociation (BIRD), collision-induced dissociation (CID), and surface-induced dissociation (SID) will create fragment ion populations with random axial phase relative to each other. Rephasing of these ions to obtain phase-coherent ion populations is absolutely necessary for the second stage mass spectrum to be acquired by ion image detection.

In the second case, ac excitation and de-excitation will also be important in preparing ion packets in known states of axial excitation and, in conjunction with variation of injection parameters that affect initial ion packet axial width, will be important in studying ion packet dephasing processes in the Orbitrap. Such studies will be important in first understanding ion packet dynamics in the Orbitrap and subsequently devising ion rephasing methods for improving Orbitrap performance, especially increasing transient time and thus resolution and mass accuracy. We also believe that these methods, especially de-excitation followed by re-excitation, may be valuable in improving resolution and ion dynamic range within the Orbitrap.

Experimental Section

Orbitrap Mass Spectrometer. The Orbitrap instrument was built by Thermo Masslab Ltd. (Manchester, U.K.). Readers unfamiliar with this type of mass spectrometer are encouraged to refer to detailed descriptions provided elsewhere.[2,6,33] A simple summary of the instrumentation and its operation follows. Ions are generated by an electrospray ionization (ESI) source and then proceed through an RF-only guide quadrupole (Q_0, $r_0 = 2.75$ mm, 2.5 MHz, 0.1−1 kV_{pp}). After passing through a second RF-only transmission quadrupole (Q_1, $r_0 = 2.22$ mm, 920 kHz, 300 V_{pp}), the ions are trapped in the storage quadrupole (Q_2, linear RF-only trap, $r_0 = 2.75$ mm, 3.45 MHz, 4100−4400 V_{pp}).

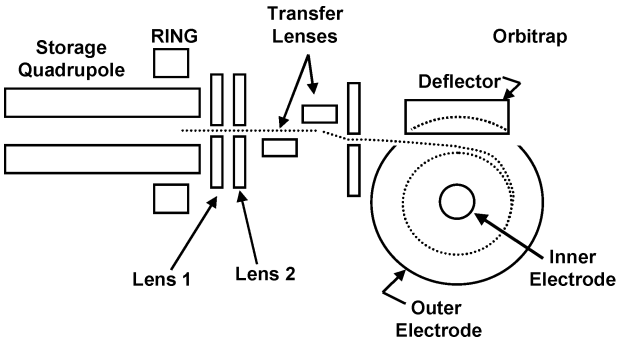

Figure 1. Schematic depiction showing storage quadrupole, lenses 1 and 2, ion transfer lenses, and the Orbitrap mass analyzer. The Orbitrap is seen end-on in this view. The dotted trace shows the ion path, starting from the storage quadrupole, through the lenses, the ion entrance slot and the deflector of the Orbitrap, and to the adoption of a stable orbit inside the Orbitrap. Not drawn to scale.

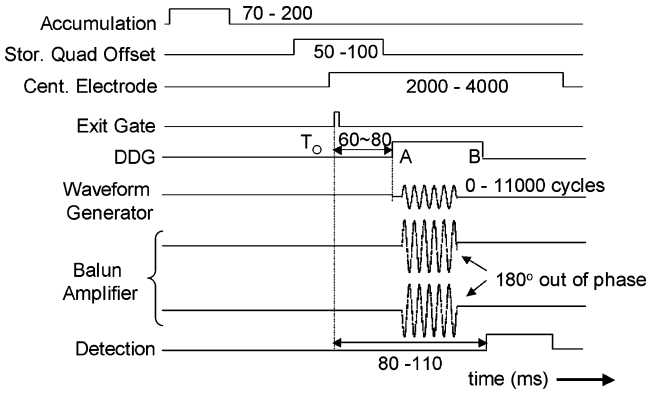

Figure 2. Timing diagram used in resonant ac de-excitation/re-excitation experiments. The accumulation, ion energizing (storage quad offset) and central electrode timing pulses were the same as in the normal Orbitrap experiment. The drive waveform was applied after the initial delay and before detection. All times in units of milliseconds. DDG is digital delay generator.

For each scan, the storage quadrupole accumulates ions for 70−200 ms and then ejects them as a single packet of ions, which arrives at the entrance to the Orbitrap with a small temporal (100−200 ns) and spatial spread (few millimeters).[33,34] The storage quadrupole is required to couple the continuous electrospray ion source with the Orbitrap, which operates in a pulsed fashion. (We note that the storage device before the Orbitrap and the mechanism of injection differ from the now-commercially available Orbitrap instrument.) Bunching is accomplished by adding a ring electrode around the exit end of the storage quadrupole rods and providing a dc-bias to this ring. The electric field from the dc-biased ring penetrates into the storage quadrupole, creating a small axial well at the exit end of the storage quadrupole. After ions are accumulated for the desired time period, the dc offset of the storage quadrupole is raised. This energizing process is described in more detail below. The storage quadrupole, transfer lenses, and Orbitrap are schematically depicted in Figure 1.

The depth of the potential well in the storage quadrupole is approximately 1% of the potential difference between the ring electrode and the dc offset of the storage quadrupole (so, for this study, ca. 5 V). Due to the loss of ion kinetic energy in collisions with the bath gas ($\sim 10^{-4}$ mbar), ions slow and accumulate in the axial well. Variation of the axial distribution of the trapped ion cloud in the Orbitrap can be achieved by prior adjustment of the depth of the potential well in the storage quadrupole, which can be done by altering the voltage on the ring electrode. A stand-alone secondary electron multiplier, located behind the Orbitrap and in line with the ion beam, can be used for detecting ion bunches when the potentials on the deflector/compensator, normally used to bend ions into the Orbitrap, and that on the Orbitrap central electrode, are switched off.

After accumulation, the ions are energized by bringing the dc offset of the storage quadrupole from near ground up to approximately 1300 V. This provides the ions with the necessary kinetic energy for assuming orbits inside the Orbitrap mass analyzer, while also allowing both the Orbitrap and the entrance quadrupoles to be operated at potentials close to ground. A typical setting for the ring electrode potential is 750 V; hence the depth of the potential well at the exit end of the storage quadrupole is about 5 V, as noted above. After the storage quadrupole dc offset is raised, the exit lens potential is changed from 1930 to −1260 V, thereby sending the ion bunch through the transfer lens system into the Orbitrap.

After traversing lenses 1−4, ions of each mass/charge ratio arrive at the entrance of the Orbitrap as short packets only a few millimeters long. For each mass/charge population, this corresponds to a spread of flight times of only a few hundred nanoseconds for mass/charge ratios of a few hundred Daltons/charge. Such durations are considerably shorter than a half-period of axial ion oscillation in the trap. When ions are injected into the Orbitrap at a position offset from its equator, these packets start coherent axial oscillations without the need for any additional excitation.

The deflector/compensator electrode at the Orbitrap is switched from 80 V during ion injection to 500 V during signal detection whereas the central electrode voltage is set at −3300 V. The signal is recorded as an image current and is typically acquired for up to 800 ms after an initial delay of ca. 110 ms and at a sampling rate of 5000 kHz. The total number of data points collected is typically 2,[22] or 4 Mpoints. The transient is Fourier transformed using the MIDAS data analysis program[3] into a mass spectrum, with no zero filling and no apodization. Signal intensities in this work refer to peak heights in the mass spectrum.

Timing of ac Dipolar Excitation/De-excitation Waveforms. Axial dipolar de-excitation and re-excitation were performed after an initial delay (60−80 ms) relative to ion injection. The initial delay is needed for *radial and angular* dephasing of the ion packets.[2] Ion image current detection was started 110 ms after ion injection. Delay of the ac waveform was controlled by a digital delay generator (DDG, Stanford Research Systems Model DG535). Figure 2 provides the timing diagram used in this experiment. The accumulation, ion energizing and central electrode timing pulses were the same as those described previously for normal scan experiments.[6] The exit gate timing pulse, which was utilized to open the gate to inject ions from the storage quadrupole into the Orbitrap, was used to trigger the DDG.

A waveform generator (model AFG320, Sony Tektronix) was activated by the DDG to create an ac waveform in the burst mode with a particular frequency and number of cycles. The bandwidth of this ac waveform in the frequency domain depends on the number of cycles according to Fourier transform theory.[35] A home-built balun amplifier was employed to produce a dipolar ac waveform, which was then applied to the split outer electrodes of the Orbitrap. The relative phase angle of the ac with respect to ion motion in the *z*-direction was controlled by varying the delay generated via the DDG. Although the DDG can completely control the relative time between ion injection and the application of an ac signal, the relative phase angle is

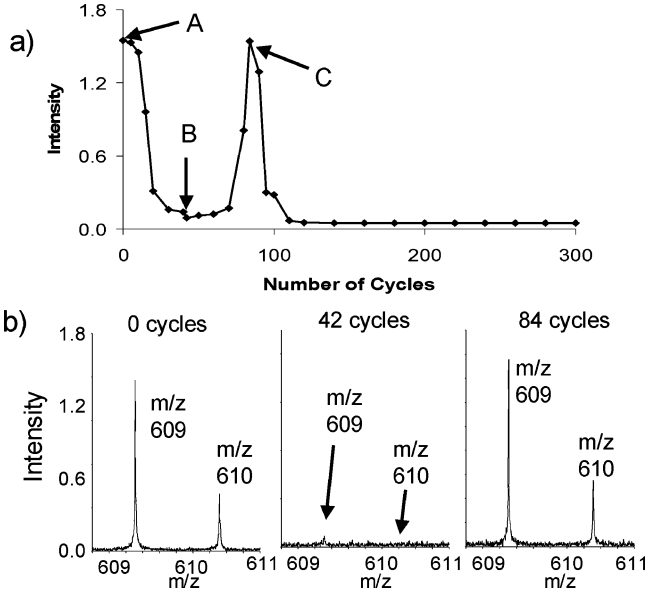

Figure 3. Demonstration of de-excitation/re-excitation of reserpine (MH^+) ions at *m*/*z* 609 when a resonant ac waveform was applied at a phase angle of 180° with respect to ion oscillation. (a) De-excitation/re-excitation curve in which the intensity of the peak at *m*/*z* 609 is plotted as a function of the number of resonant ac cycles applied. (b) Three actual mass spectra, corresponding to points A, B, and C on the de-excitation/re-excitation curve, which are respectively the normal Orbitrap mass spectrum without ac applied, the fully de-excited mass spectrum and the fully re-excited mass spectrum.

subject to a small drift. This may be due to (i) drift in the frequency of ion oscillation in the Orbitrap from scan to scan or (ii) time jitter in the arrival of ions at the Orbitrap or possibly both effects. A phase lock circuit may provide better control in future experiments.

Reagents and Electrospray Conditions. All chemicals used were purchased from Sigma (St. Louis, MO) and dissolved in water/methanol (50:50 v%:v%) with 0.1% (v%) formic acid. The concentrations were 0.02 mg/mL for reserpine and 0.1 mg/mL for angiotensin. The samples were introduced into the electrospray source at a flow rate of 5 μL/min using a syringe pump (Harvard, South Natick, MA). Typically, the ESI capillary was held at 3000 V and 150 °C.

Results and Discussion

Axial De-excitation/Re-excitation and Ejection. De-excitation/re-excitation of axial motion using a resonant ac waveform was followed by measuring ion signal intensity vs the number of ac cycles applied. The intensities of the reserpine ion (MH^+) at *m*/*z* 609 were used in this work, except when otherwise indicated. The frequency of harmonic motion in the *z*-direction for this ion is 447.2 kHz for the experimental settings used here. Figure 3a shows an example of de-excitation/re-excitation. Each point on this curve was obtained by recording a separate 800 ms transient. The dipolar ac had an amplitude of 20 V_{pp} and was applied at a phase angle of 180° with respect to the oscillation of the trapped ions. Upon application of the ac waveform, the ion signal initially drops, reaching a minimum at about 42 cycles, and then starts to rise again. At 84 cycles, the signal reaches a maximum comparable to the original signal and then diminishes to the noise level, not increasing again even after 300 cycles of ac were applied.

Three actual mass spectra, shown in Figure 3b, correspond to points A, B, and C on the excitation curve. The peak intensities at points A and C are nearly identical, the former is due to the original mass spectrum and the latter is due to the fully *re-excited* signal. The mass spectrum for point B represents the almost fully de-excited signal, the peak at *m*/*z* 609 being close to the noise level. Note that the isotopic peak at *m*/*z* 610 has been de-excited and re-excited at the same time as the peak at *m*/*z* 609 in this experiment.

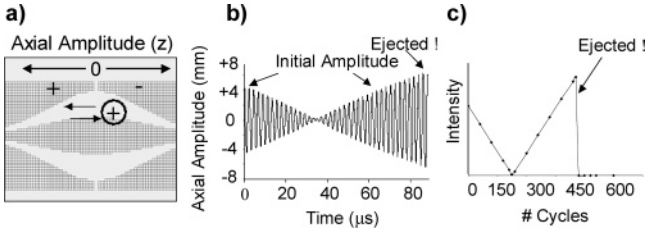

Figure 4. Simulation results for a resonant ac waveform applied 180° with respect to ion oscillation. (a) Schematic depiction of outer electrode polarity required to achieve 180° phase relative to a positive ion. Electrodes drawn by SIMION. The outer electrode is split at the equator, the central plane in the Orbitrap ($z = 0$). (b) SIMION simulation results for axial position vs time for a single ion undergoing resonant ac excitation. (c) ITSIM simulation results of peak intensity as a function of number of cycles of applied ac, analogous to Figure 3a, for a single ion system.

Trapped ions in the Orbitrap undergo oscillation in the *z*-direction with a frequency dependent only on mass/charge ratio (eq 2) and an amplitude determined by the injection offset from the equator. The ion image current for a population of ions of given *m*/*z* ratio will be proportional to the total number of ions and their amplitude in the z-direction (eq 3). Figure 4 uses simulations to follow ion motion in the Orbitrap when the phase angle of the resonant ac is 180° out of phase with respect to the ion oscillation. When a resonant ac waveform is applied, ions of the appropriate *m*/*z* ratio experience a force in the direction opposite to their axial motion, causing the axial amplitude to decrease with the number of cycles of ac applied, diminishing to zero after a given number of cycles. Correspondingly, as the ions' *z*-amplitudes decrease, so will the ion image signal, which is proportional to the ions' axial amplitudes. Thus, it is this decrease in the ions' *z*-amplitudes that is responsible for the decrease in the plot from point A to point B.

Once the ions have reached very small axial amplitudes, they can only be accelerated by the ac and, therefore, at this point, will take on the *same phase* as the applied ac waveform (i.e., 0° relative phase). At this point, their axial amplitude starts to increase. The rise in the plot from point B to point C is due to the increasing amplitude of axial oscillation, as eq 3 predicts. Ultimately, if the ac waveform is continued, the ions will gain even more axial energy and increase their *z*-amplitude beyond the bounds of the Orbitrap and impact the outer electrode. The ejection process of the ion populations causes the decrease from point C to 125 cycles in Figure 3. Alternatively, if the ac phase is changed by 180° at point C, the ions undergo a new round of de-excitation followed by re-excitation (data not shown). In practice, the cycle of de- and re-excitation could be repeated an arbitrary number of times, so long as the ac phase is changed by 180° every time the equivalent of point C is reached.

Both the reserpine ion at *m*/*z* 609 and the $^{13}C_1$ isotopic ion at *m*/*z* 610 showed de-excitation/re-excitation at the same number of cycles of the applied ac waveform in this experiment. Although the resonant frequency of the isotopic ion was not 447.2 kHz, the ions at *m*/*z* 610 were affected by the same ac waveform nonetheless, because this ac waveform has a rather broad bandwidth in the frequency domain. (We will discuss this more fully in a later section.) It should also be noted that the ac waveform is applied when *m*/*z* 609 and 610 are in phase with

each other. As their oscillation frequencies are slightly different, 447.2 and 446.8 kHz, respectively, one must also adjust the ac waveform trigger to a point when both populations are in phase with each other.

Similar results were acquired when a smaller amplitude (3.8 V_{pp}) ac waveform was used. The number of cycles of ac needed to reduce the intensity of the peak to baseline was now much greater, 250, as was the total number of cycles needed to reestablish the initial level, 470. In this paper, we will adopt the convention of reporting *total* number of ac cycles needed to achieve re-excitation. So, for example, in this case, 250 cycles were needed to obtain complete de-excitation. An *additional* 220 cycles from that point were required to reach re-excitation, for a *total* number of 470 cycles. In a similar experiment, de-excitation/re-excitation of the singly charged angiotensin ion (MH^+) at nominal *m*/*z* 1296 Th was achieved using a dipolar ac of 4.1 V_{pp} and a resonant frequency of 306.5 kHz. About 200 cycles of ac were required to de-excite this peak to the noise level and 420 cycles were needed to achieve full re-excitation. After 420 cycles, the intensities of the peak at *m*/*z* 1296 decreased to the noise level and this peak did not reappear even after 1100 cycles of resonant ac, a result that is again consistent with complete ejection of all the ions.

The above interpretation of the de-excitation/re-excitation experiment in the Orbitrap is qualitatively consistent with both SIMION and ITSIM simulations. Parts b and c of Figure 4 show simulations depicting how the axial amplitude of ion motion (Figure 4b) and the peak intensity (Figure 4c) change as functions of time when a resonant ac signal (40 V_{pp}) is applied at a phase angle of 180°. As the ion axial amplitude decreases from its initial value as the ac is applied, the peak height drops correspondingly. Both the ion axial amplitude and ion peak height reach a minimum after some number of ac cycles; this value depends on the strength of the applied ac. Once the minimum ion axial excursion and peak height are reached, ion axial motion rephases and assumes the phase of the applied ac signal. From this point, the amplitude of ion motion increases, thereby causing the ion peak in the mass spectrum to grow larger. The amplitudes of ion motion and the ion signal reach their initial values and maintain these values if the application of the dipolar ac signal is stopped at this point. If the ac signal continues to be applied, ion axial motion is driven to larger amplitudes, with the eventual outcome that the ions are ejected from the Orbitrap and ion signal drops to zero. This is shown by the portion of Figure 3 from point C onward.

De-excitation/re-excitation has been demonstrated, as expected, in this experiment. However, we have assumed that the entire population of trapped ions of a given *m*/*z* ratio is moving in phase axially and that it occupies an infinitely small width in the axial direction. As noted earlier, the axial size of the stored ion cloud can be manipulated by adjusting the ring electrode voltage. The effect of this adjustment on de-excitation/re-excitation is examined in more detail in a later section.

Excitation/Ejection. In contrast to the previous experiment, the ac waveform can be applied *in phase* with ion motion (i.e., relative phase angle of 0°), leading to rather different behavior. Figure 5 shows this experiment with ac amplitude of 3.8 V_{pp}. The peak height decreases immediately and very rapidly with increasing number of applied ac cycles, a result interpreted from simulations as a consequence of ion ejection. Similar results have been acquired when weaker drive waveforms are used; such as the case when the amplitude of the waveform is 0.16 V_{pp} (experiment not shown). The amplitude of the drive

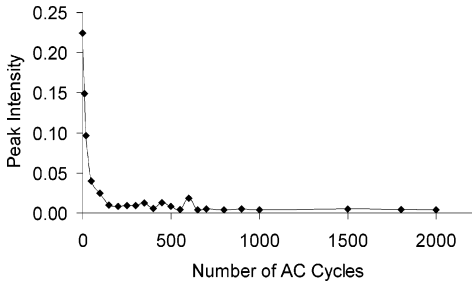

Figure 5. Ejection of reserpine ion at *m*/*z* 609 when a resonant ac waveform, with amplitude 3.8 V_{pp}, was applied in phase with the oscillation of trapped ions. With increasing number of cycles applied, the peak intensity drops quickly to the noise level. At this point all ions of *m*/*z* 609 have been ejected.

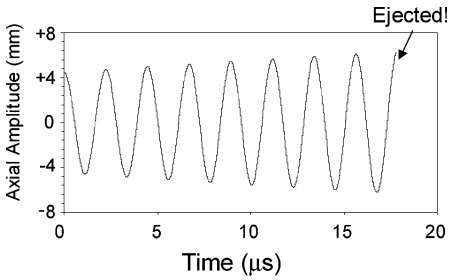

Figure 6. Amplitude of ion axial harmonic motion as a function of time when the resonant ac signal is applied in phase with ion motion. Ions pick up energy and increase their axial amplitude until it is large enough for ions to be ejected.

waveform does not make any difference except to increase the number of cycles required to eject the ion packet and fully lose the peak.

Resonance ejection is based on the fact that ion axial motion in the Orbitrap will be excited to higher amplitude when a resonant ac waveform is applied in phase with the ion motion. Once the ions acquire sufficient energy, they will be ejected. Figure 6 shows the SIMION simulation results, in which the axial amplitude of a stored ion increases in phase with the applied ac (40 V_{pp}) until it is ejected. As the application of the ac results in a larger amplitude of ion motion, it might be expected that a slight increase in ion image current would be observed at small numbers of ac cycles, before the ion peak height rapidly decreases. This may be verified by recalling that the ion image current is proportional to the *z*-amplitude of the ions,[2] which is being increased by this experiment. Contrary to this expectation, Figure 5, the plot of the experimental data, shows that the peak intensity drops directly to the noise level when the ac is applied. We surmise that the ion packet (of *m*/*z* 609) occupies a distribution of axial positions sufficiently large that the ac signal causes a fraction of the ions to be ejected almost immediately. This loss of ions offsets any gain in image signal due to increased amplitude at small numbers of cycles. The ejection process then continues as more cycles of ac are applied.

Frequency Effects on De-excitation. An important characteristic of resonance excitation is how changes in the frequency of the drive waveform affect the de-excitation/re-excitation of an ion population. Figure 7 shows the results of two experiments. Each frequency response curve (signal intensity as a function of applied ac frequency) is plotted for an ac phase angle of 180° and constant ac amplitude and number of cycles. For each curve, the number of cycles was held constant and corresponds to full de-excitation of the ion population at resonance. Figure 7a illustrates responses for both the reserpine MH^+ ion at *m*/*z* 609 and its $^{13}C_1$ isotopic peak at *m*/*z* 610. The ac amplitude

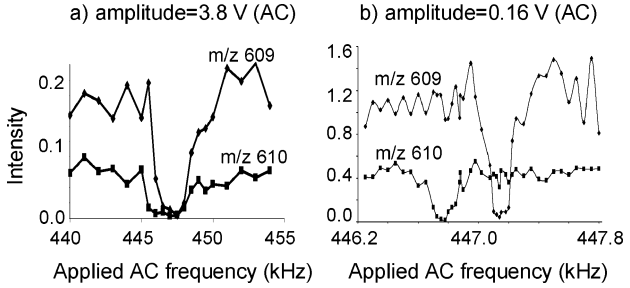

Figure 7. Frequency response (resonance) curves of the reserpine monoisotopic ion MH^+ at *m*/*z* 609 and the $^{13}C_1$ isotope at *m*/*z* 610. In both cases, the phase of the applied ac wave is 180° relative to ion motion. (a) Response to broad-band ac waveform (3.8 V_{pp}, 250 cycles, corresponding to bandwidth of 3.6 kHz as measured at baseline). (b) Response to narrowband ac waveform (0.16 V_{pp}, 5500 cycles, 0.16 kHz bandwidth).

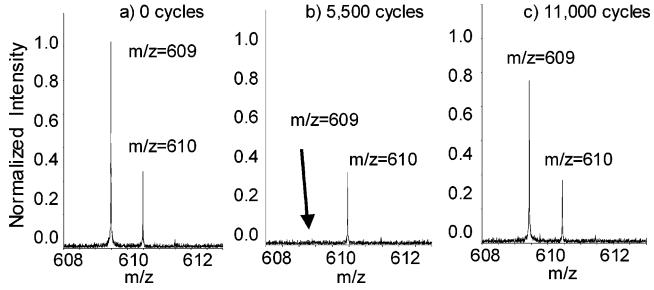

Figure 8. Mass-selective de-excitation/re-excitation of reserpine ion at *m*/*z* 609 without disturbing the isotopic ion population at *m*/*z* 610 using 0.16 V_{pp} ac with a phase angle of 180°: (a) 0 cycles of ac applied; (b) 5500 cycles applied for 12 ms; (c) 11 000 cycles applied 25 ms. The vertical scale is the same for all three mass spectra.

was 3.8 V_{pp}, and the number of cycles used was 250. The intensities for these two peaks show no response to the frequency of the ac until near their harmonic oscillation frequencies, 447.2 kHz for *m*/*z* 609 and 446.8 kHz for *m*/*z* 610. Note that the resonant frequency of the isotopic peak at *m*/*z* 610 is lower than that for *m*/*z* 609, as predicted by eq 2. However, using these large ac amplitudes results in substantial overlap between these two ions' resonance peaks and thus very little resolution.

Figure 7b portrays a similar experiment but where an ac signal of lower amplitude, 0.16 V_{pp} was used and where 5500 cycles were required for complete de-excitation. The intensity of the isotopic peak at *m*/*z* 610 begins to drop at a lower frequency and remains at the minimum value over a narrower frequency range compared to Figure 7a, before returning to its original intensity. The intensity of the peak at *m*/*z* 609 now achieves its minimum at a distinctly higher frequency than does that of *m*/*z* 610. This demonstrates that ion populations at *m*/*z* 609 and 610 can be selectively de-excited, leaving one or other ion population intact, provided the ac waveform's central frequency and bandwidth are chosen appropriately.

Applying ac signals with higher amplitudes means that a smaller number of ac cycles is required to fully de-excite an ion population, which implies that this kind of ac has a narrower width in the time domain and correspondingly a wider distribution in the frequency domain.[35] For example, only 250 cycles were needed to de-excite the ions at *m*/*z* 609 when the amplitude of the drive waveform was 3.8 V_{pp}. The bandwidth of this signal was 3.6 kHz (at baseline) in the frequency domain. Therefore, because the frequency of the isotopic ion at *m*/*z* 610 is 446.8 kHz and the difference from 447.2 kHz is only 0.4 kHz, this waveform was wide enough to de-excite both sets of ions simultaneously. However, a waveform with a frequency of 447.2 kHz and amplitude of 0.16 V_{pp} that is applied for 5500 cycles corresponds to only 0.16 kHz in bandwidth. Thus, in this case, the ion population at *m*/*z* 609 can be fully de-excited whereas the isotopic ion at 610 is unaffected.

Mass-Selective De-Excitation/Re-Excitation. The results just described suggested that de-excitation/re-excitation could be carried out in a mass selective fashion, even for isotopic ions. Figure 8 summarizes the results of mass-selective de-excitation/re-excitation of reserpine ions at *m*/*z* 609 using an ac signal with the low amplitude of 0.16 V_{pp} applied for 0, 5500 and 11 000 cycles, at a phase angle of 180° with respect to the original axial ion motion. Figure 8a depicts the initial signal with no ac utilized, and it includes the main peak at *m*/*z* 609 and the isotopic peak at *m*/*z* 610.

Shown in Figure 8b is the mass spectrum recorded after 5500 cycles of ac had been applied to de-excite the reserpine ion at *m*/*z* 609. Note that only the peak at *m*/*z* 609 has disappeared whereas the isotopic peak at *m*/*z* 610 maintained its intensity. This result should be contrasted with the de-excitation/re-excitation experiment discussed in Figure 3, in which both the monoisotopic and $^{13}C_1$ isotopic peaks were completely de-excited by applying 42 cycles of a dipolar ac with an amplitude of 20 V_{pp} (bandwidth of 20 kHz). Figure 8c displays the re-excited signal after 11 000 cycles of ac. Peaks at *m*/*z* 609 and 610 have almost the same intensities as in the original mass spectrum and peak widths are very similar.

It is interesting to estimate the resolution of de-excitation (R_{de-exc}) obtained in Figure 8b. This value is given by $R_{de-exc} = m/\Delta m = 2740$, with Δm given by one-half the bandwidth of the de-excitation signal, 0.08 kHz, divided by 0.36 kHz, the spacing between adjacent integral mass-to-charge ratios at *m*/*z* 609. It is instructive to compare this value for R_{de-exc} with the resolution obtained for the direct excitation and ejection of the same *m*/*z*, R_{eject}. In an experiment like that of Figure 5, *m*/*z* 609 was ejected at approximately 4000 cycles at 0.16 V_{pp} (data not shown), resulting in $R_{eject} = 1960$. Although the results are similar in magnitude, the nearly 40% difference between R_{de-exc} and R_{eject} underscores the different physical processes involved and suggests that initial ion axial amplitude must be great enough that excitation and ejection occurs more quickly than de-excitation.

Besides the experiment shown above, in which the three mass spectra displayed are derived from three separate transients, mass-selective de-excitation/re-excitation experiments can also be performed in a more integrated fashion. For example, both the de-excitation and re-excitation ac waveforms can be applied well after image current detection has started. Because of the time of ac application, these waveforms themselves appear in the recorded ion image current transients. The first ac waveform, applied out of phase with respect to ion motion, is used to mass-selectively de-excite the trapped axially oscillating ion population and the second ac waveform is used to re-excite these ions mass-selectively.

Figure 9a shows the transient signal recorded for this experiment when a mixture of reserpine and angiotensin was electrosprayed. Detection started 80 ms after ion injection and the two ac waveforms (447.2 kHz, 3.8 V_{pp}, 250 cycles each, labeled "first ac" and "second ac" in Figure 9a) were applied 100 ms and 340 ms after detection was started. Detection continued for 800 ms. The two ac waveforms divide the transient into three periods. These three segments of the transient (labeled A, B and C) were individually Fourier transformed and the corresponding mass spectra are shown in Figure 9b−d. The mass spectra in Figure 9b,d, containing the reserpine peak at *m*/*z* 609, doubly charged angiotensin $(MH_2)^{2+}$ at *m*/*z* 649 and all relevant

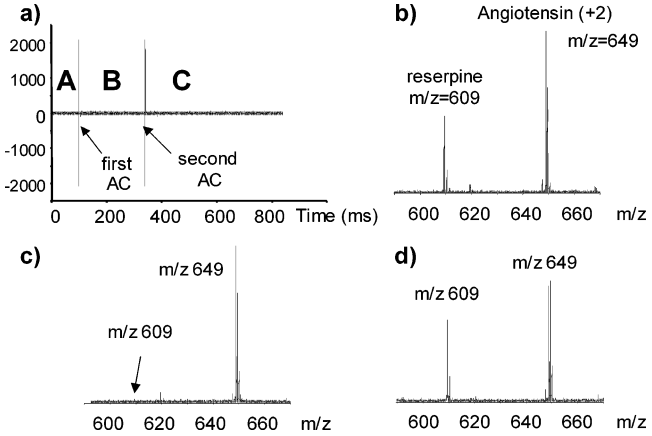

Figure 9. Selective de-excitation/re-excitation of reserpine ion at *m*/*z* 609 without affecting doubly charged angiotensin ions at *m*/*z* 649. Two ac waveforms (447.2 kHz, 3.8 V_{pp}, 250 cycles each, 0.56 ms) were applied separately after the image current detection was started. (a) The recorded signal from the split outer electrode of the Orbitrap showing the transient region A, the first ac waveform, the transient region B, the second ac waveform and the transient region C. Note that the ion signals are much smaller than the applied ac waveforms. (b) Fourier transform mass spectrum corresponding to transient segment A, normal mass spectrum before application of an ac waveform. (c) Mass spectrum corresponding to transient segment B, after application of the first ac waveform and resultant de-excitation of *m*/*z* 609 and loss of 609 ion signal with retention of *m*/*z* 649 signal. (d) Mass spectrum corresponding to transient segment C, reserpine peaks re-excited by the second ac waveform applied.

isotopic peaks, are nearly identical. In Figure 9c, only the angiotensin peak at *m*/*z* 649 was observed, even though the reserpine ions were present in the trap and could be made visible by application of the second ac waveform.

Clearly, the first part of this transient (region A) describes ion motion that has not been disturbed by the ac and thus the corresponding mass spectrum is a normal Orbitrap signal, albeit recorded using a relatively short detection time (100 ms). The first ac waveform is used to de-excite reserpine peaks to the equatorial plane of the Orbitrap ($z = 0$). After the second ac waveform was applied, reserpine ions, previously de-excited to the equatorial plane by the first ac waveform, acquired the phase of this second ac and were axially re-excited.

The height of the reserpine peak in Figures 9d (re-excited ions) is slightly greater than the reserpine peak in Figure 9b (ions before de-excitation). This three-region transient experiment suggests that ions can be de-excited to the central plane of the Orbitrap, survive for some time and then be re-excited to regain the full *z*-amplitude. Moreover, the experiment shows that re-excitation to the same, or possibly even slightly greater, axial amplitude is possible. Comparison of magnitudes between these mass spectra is meaningful because (i) the mass spectra in Figures 9b−d are all Fourier transformed from time domain segments of the same length (90 ms) and (ii) all three spectra are of the same ion population. Interestingly, the angiotensin peak in Figure 9b is only very slightly more intense than that in Figure 9c, and considerably more intense than the peak in 9d. The difference in height, especially between Figure 9b,d may be indicative of the decrease in ion signal due to dephasing processes such as collisions with background gases.

Phase Relationship between Ion Motion and the Applied ac Waveform. The consequences of the application of an ac signal depend on its phase angle with respect to the ion motion, as the two special cases of 0° and 180° have illustrated. The full phase delay curve, a plot of peak intensity as a function of delay time between injection and activation, was also investigated. In this experiment, adjustment of the relative phase angle was accomplished by delaying the triggering time of the ac waveform. Figure 10 displays the phase delay curve of the reserpine ion at *m*/*z* 609 when the drive waveform was 470 cycles of ac with amplitude 3.8 V_{pp}. With increasing delay time, the peak height increases and decreases periodically.

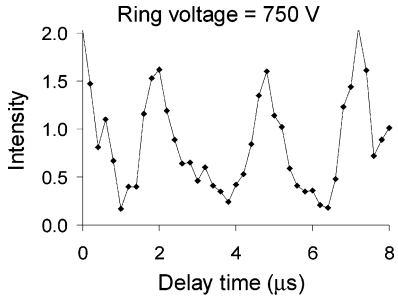

Figure 10. Phase delay curve, a plot of peak intensity of reserpine ion at *m*/*z* 609 as a function of delay time between injection and activation, in which the relative phase angle, controlled by the delay time, was adjusted by triggering the ac signal at different times. The ac applied here had an amplitude of 3.8 V_{pp} and 470 cycles. The peak intensity increased and decreased periodically with the change of the delay time. The frequency of increase and decrease of the peak intensity is approximately the frequency of ion oscillation at *m*/*z* 609 in the Orbitrap.

The length of the delay time between injection and the point at which the dipolar ac was applied was critical in this experiment, as it controlled the phase. By variation of the length of the delay, the peak intensity went through maxima when the ac phase was 180° with respect to initial ion motion. Each maximum in Figure 10 corresponds to the point C in Figure 3, fully re-excited ion axial motion. In Figure 10, minima appear approximately midway between the maxima. This is consistent with those delay times corresponding to a relative ac waveform phase of 0° (analogous to nearly any point after the initial decrease in Figure 5). The spacing between maxima is roughly equal to the resonant frequency of the reserpine ion.

Conclusions

These experiments demonstrate that ions confined in the Orbitrap can be de-excited and re-excited resonantly in a mass-selective or a broad-band fashion. The stored ions can be mass-selectively de-excited to the central plane of the Orbitrap, re-excited to be observed with regained signal strength, and ejected if the ac is applied 180° with respect to the initial ion oscillation. Phase delay curves show that ion signal intensity increases and decreases periodically with the change of phase relationship between the applied ac and the ion oscillation. These preliminary results also qualitatively compare well with computer simulations using SIMION and ITSIM. Such comparisons will be detailed in a future paper.

The techniques of resonant de-excitation and resonant ejection appear to be broadly applicable. The demonstrated mass/charge range of the Orbitrap is *m*/*z* 100 to *m*/*z* 6000, with corresponding frequencies of 1.1 MHz down to 142 kHz. Such frequencies are readily produced at sufficient amplitude by commercially available sources, and SWIFT waveforms can be readily constructed and applied. Under the conditions studied, resolution of de-excitation is about 40% greater than the resolution of ejection for the same amplitude waveform. The selection of either method to eliminate peaks in the mass spectrum may ultimately depend not only on the resolution but also on whether the ions of interest will be wanted in the Orbitrap for the rest of the experiment in question.

Future work will include efforts to use the ion control experiments discussed here to perform collisional activation and surface-induced dissociation as ion activation methods in MS/MS experiments. Tasks of interest include application of short axial dc pulses to activate the trapped ions to collide with the electrodes and then to trap and rephase the product ions. Furthermore, tomography experiments are planned to diagnose the spatial and velocity distributions of the trapped ions to more thoroughly understand ion motion in the Orbitrap.

Acknowledgment. This work was supported by National Science Foundation Grant CHE-0216239 (Major Research Instrumentation Program), the Office of Naval Research (ONR), and Thermo Electron Corporation. We also acknowledge Guangxiang Wu for help with the ITSIM simulations including Figure 4c, technical advice and assistance from Jason Duncan, Andy Guymon, Dr. Robert Santini, and Chris Doerge of the Jonathan Amy Facility for Chemical Instrumentation, and from Mark Hardman of Thermo Electron Corporation.

References and Notes

(1) Kingdon, K. H. *Phys. Rev* **1923**, *21*, 408−418.
(2) Makarov, A. *Anal. Chem.* **2000**, *72*, 1156−1162.
(3) Senko, M.; Canterbury, J.; Guan, S.; Marshall, A. *Rapid Commun. Mass Spectrom.* **1996**, *10*, 1839−1844.
(4) Marshall, A. G.; Verdun, F. R. *Fourier Transforms in NMR, Optical, and Mass Spectrometry: A User's Handbook*; Elsevier: Amsterdam, 1990.
(5) Makarov, A.; Denisov, E.; Lange, O.; Kholomeev, A.; Horning, S. *Proceedings of the 53rd ASMS Conference on Mass Spectrometry and Allied Topics, San Antonio, TX;* 2005.
(6) Hu, Q.; Noll, R. J.; Li, H.; Makarov, A.; Hardman, M.; Cooks, R. G. *J. Mass Spectrom.* **2005**, *40*, 430−443.
(7) Major, F. G.; Dehmelt, H. G. *Phys. Rev.* **1968**, *170*, 91−107.
(8) Guan, S.; Marshall, A. G. *Anal. Chem.* **1993**, *65*, 1288−1294.
(9) Fulford, J. E.; Hoa, D.-N.; Hughes, R. J.; March, R. E.; Bonner, R. F.; Wong, G. J. *J. Vac. Sci. Technol.* **1980**, *17*, 829−835.
(10) Louris, J. N.; Cooks, R. G.; Skya, J. E. P.; Kelley, P. E.; Stafford, G. C.; Todd, J. F. J. *Anal. Chem.* **1987**, *59*, 1677−1685.
(11) March, R. E.; Londry, F. A.; Alfred, R. L.; Todd, J. F. J.; Penman, A. D.; Vedel, F.; Vedel, M. *Int. J. Mass Spectrom. Ion Processes* **1991**, *110*, 159−178.
(12) March, R. E.; McMahon, A. W.; Londry, F. A.; Alfred, R. L.; Todd, J. F. J.; Vedel, F. *Int. J. Mass Spectrom. Ion Processes* **1989**, *95*, 119−156.
(13) Lammert, S. A.; Cooks, R. G. *Rapid Commun. Mass Spectrom.* **1992**, *6*, 528−530.
(14) Weber-Grabau, M.; Kelley, P. E.; Bradshaw, S. C.; Hoekman, D. J. *Proceedings of the 36th ASMS Conference on Mass Spectrometry and Allied Topics, San Francisco, CA*; **1988**; p 1106.
(15) McLuckey, S. A.; Goeringer, D. E.; Glish, G. L. *J. Am. Soc. Mass Spectrom.* **1991**, *2*, 11−21.
(16) Schwartz, J. C.; Jardine, I. *Rapid Commun. Mass Spectrom.* **1992**, *6*, 313−317.
(17) Liere, P.; March, R. E.; Blasco, T.; Tabet, J.-C. *Int. J. Mass Spectrom. Ion Processes* **1996**, *152*, 101−117.
(18) Murrell, J.; Despeyroux, D.; Lammert, S. A.; Stephenson, J. L.; Goeringer, D. E. *J. Am. Soc. Mass Spectrom.* **2003**, *14*, 785−789.
(19) Julian, J. R. K.; Cooks, R. G. *Anal. Chem.* **1993**, *65*, 1827−1833.
(20) Paradisi, C.; Todd, J. F. J.; Traldi, P.; Vettori, U. *Org. Mass Spectrom.* **1992**, *27*, 251−254.
(21) Weil, C.; Wells, J. M.; Wollnik, H.; Cooks, R. G. *Int. J. Mass Spectrom.* **2000**, *194*, 225−234.
(22) Cooks, R. G.; Cleven, C. D.; Horn, L. A.; Nappi, M.; Weil, C.; Soni, M. H.; Julian, R. K. J. *Int. J. Mass Spectrom. Ion Processes* **1995**, *146/147*, 147−163.
(23) Lammert, S. A.; Cleven, C. D.; Cooks, R. G. *J. Am. Soc. Mass Spectrom.* **1994**, *5*, 29−36.
(24) Cleven, C. D.; Cooks, R. G.; Garrett, A. W.; Nogar, N. S. *J. Phys. Chem.* **1996**, *100*, 40−46.
(25) Lammert, S. A.; Cooks, R. G. *J. Am. Soc. Mass Spectrom.* **1991**, *2*, 487−451.
(26) Goeringer, D. E.; Crutcher, R. I.; McLuckey, S. A. *Anal. Chem.* **1995**, *67*, 4164−4169.
(27) Syka, J. E. P.; Fies, W. J. U.S. Patent 4,755,670, 1980.
(28) Parks, J. H.; Plollack, S.; Hill, W. J. *J. Chem. Phys.* **1994**, *101*, 6666−6685.
(29) Soni, M.; Frankevich, V.; Nappi, M.; Santini, R. E.; Amy, J. W.; Cooks, R. G. *Anal. Chem.* **1996**, *68*, 3314−3320.
(30) Dahl, D. Idaho National Engineering Laboratory, 2001.
(31) Bui, H. A.; Cooks, R. G. *J. Mass Spectrom.* **1998**, *33*, 297−304.
(32) Plass, W. R.; Li, H. Y.; Cooks, R. G. *Int. J. Mass Spectrom.* **2003**, *228*, 237−267.
(33) Hardman, M.; Makarov, A. *Anal. Chem.* **2003**, *75*, 1699−1705.
(34) Makarov, A.; Hardman, M.; Schwartz, J.; Senko, M., International Patent, WO 02/078046 A2, 2002.
(35) Bracewell, R. N. *The Fourier Transform and its Applications*, 3rd ed.; McGraw-Hill: Boston, 2000.